Bilal M. Ayyub
Center for Technology and Systems Management,
Department of Civil and Environmental Engineering,
University of Maryland,
College Park, MD 20742

Karl A. Stambaugh
Naval Architect,
United States Coast Guard Surface Forces Logistics Center,
Baltimore, MD 21226

Timothy A. McAllister
Naval Architect,
United States Coast Guard Surface Forces Logistics Center,
Baltimore, MD 21226

Gilberto F. de Souza
Department of Mechatronics and Mechanical Systems Polytechnic School,
University of São Paulo,
São Paulo 05508-900, Brazil

David Webb
Center for Technology and Systems Management,
Department of Civil and Environmental Engineering,
University of Maryland,
College Park, MD 20742

Structural Life Expectancy of Marine Vessels: Ultimate Strength, Corrosion, Fatigue, Fracture, and Systems

This paper provides a methodology for the structural reliability analysis of marine vessels based on failure modes of their hull girders, stiffened panels including buckling, fatigue, and fracture and corresponding life predictions at the component and system levels. Factors affecting structural integrity such as operational environment and structural response entail uncertainties requiring the use of probabilistic methods to estimate reliabilities associated with various alternatives being considered for design, maintenance, and repair. Variability of corrosion experienced on marine vessels is a specific example of factors affecting structural integrity requiring probabilistic methods. The Structural Life Assessment of Ship Hulls (SLASH) methodology developed in this paper produces time-dependent reliability functions for hull girders, stiffened panels, fatigue details, and fracture at the component and system levels. The methodology was implemented as a web-enabled, cloud-computing-based tool with a database for managing vessels analyzed with associated stations, components, details, and results, and users. Innovative numerical and simulation methods were developed for reliability predictions with the use of conditional expectation. Examples are provided to illustrate the computations. [DOI: 10.1115/1.4026396]

Keywords: corrosion, fatigue, fracture, life expectancy, infrastructure, risk, ships, strength, structure, system, ultimate strength

1 Background

Ship structural adequacy considerations require reliability assessments to support engineering, operational, and maintenance decisions based on risk and benefit trade-offs. The structural adequacy considerations include the ultimate hull girder strength based on stiffened panel structural configurations, fatigue, and fracture life predictions. Effects of homeport rotations on structural fatigue loading and corrosion are subject to variability that is describable only in probabilistic terms. Factors affecting structural integrity such as operational environments and structural responses entail uncertainties requiring the use of probabilistic methods to estimate reliabilities associated with various alternatives being considered for design criteria, maintenance, and repair. For example, the variability of corrosion experienced by vessels is one of the factors affecting structural integrity requiring a probabilistic treatment.

Reliability and life expectancy analysis are typically based on particular failure modes at the component and system levels. The following primary failure modes with corrosion effects are considered in this paper: (1) failure of a hull girder as a stiffened thin-walled structure by reaching its ultimate strength; (2) failure of a stiffened panel by material yielding or instability of one or a group of its components; (3) fatigue of structural details due to cyclic loading; and (4) fracture of a member. Numerical and simulation methods are typically used for assessing the time-dependent reliabilities for these failure modes.

Manuscript received January 25, 2014; final manuscript received October 13, 2014; published online February 27, 2015. Assoc. Editor: James Lambert.

The first and second failure modes are based on ultimate strength and extreme loading conditions with corrosion consideration that degrade strengths of the hulls and members. These two failure modes require the use of extreme value analysis and first-crossing time-dependent reliability analysis. These modes were investigated extensively for marine vessels, bridge girders, and other similar structures [e.g., 1,2].

The fatigue performance of marine vessels has been an area of interest and investigation using the stress cycles to failure (i.e., S-N) cumulative damage fatigue analysis [3]. The S-N formulation provides a prediction of fatigue life based on defining failure by crack initiation. Fracture mechanics methods assess life based on crack propagation from an initial crack size to full penetration in a structural member. A combination of fracture mechanics and stochastic modeling of loads provides the necessary tools for these reliability calculations. A limit state function can be formulated by applying linear elastic fracture mechanics. The uncertainties of key influencing parameters can be taken into account by treating them as basic random variables. Such methods should account for corrosion effects on member thicknesses and geometry. Additionally, a fracture mechanics approach produces crack size distribution associated with a vessel's operational life and use [4].

Examining the hull girder of a vessel as a system entails the reliability analysis of hundreds of components in terms of ultimate strength, fatigue, and fracture with spatial and environmental exposure correlations. The reliability of the system can be approximated based on a discretized vessel in the form of a hull girder, stiffened panels, fatigue details, and fracture locations at critical regions. Weakest link modeling for system reliability forms a practical basis for assessing the time-dependent reliability of the system.

This system modeling formulation can account for interdependence among the components based on the assumption of either perfect dependence or independence using bounding methods for system reliability assessment.

Reliability and life expectancy analysis of marine vessels requires the management of voluminous and potentially dispersed information. The management in this case can be facilitated by the use of web-enabled databases and analytical tools. With the support of the U.S. Coast Guard (USCG), BMA Engineering, Inc. (BMA) developed the Structural Life Assessment of Ship Hulls (SLASH) methodology to compute the time-dependent reliability functions for hulls, stiffened panels, fatigue details, and fracture at the component and system levels [5]. SLASH requires specification of the basic random variables for the corresponding performance functions representing a structural failure mode. BMA has developed a tool that implements the SLASH methodologies. This web-enabled, cloud-computing-based tool with a database can be used to manage ships analyzed and associated stations, components, details and results, and users. The methods are illustrated using examples with insightful observations in this tool.

In this paper, the reliability and life expectancy analysis methodology is fully developed and illustrated using a USCG cutter. This type of analysis is being used to support decision making for maintenance, operation, and repair as part of fleet support and hull structural life evaluations for the USCG's aging legacy cutters and recapitalization of new cutters. The assessments are being used as a basis for making statements relating to the structural life based on the probability of failure for a critical location, groupings of similar structural components, and critical regions of a vessel.

2 Component Reliability Analysis

2.1 Introduction. The methodology proposed in this paper is presented at two levels, the component level and the system level. The component level produces time-dependent reliability functions for hulls, stiffened panels fatigue, and fracture. The system level aggregates the results from the component-level analyses to produce time-dependent reliability functions for a particular group (or groups) of components treating the system as in series, i.e., with a weakest link, to compute the system reliability.

This section presents the methods for assessing the reliability at the component level. The components are defined by structural performance functions for potential failure modes including the ultimate collapse of a hull, the ultimate failure including buckling of a stiffened panel, the fatigue failure of a structural detail, and the fracture of a structural member. For each failure mode, the methodology produces a time-dependent reliability function. The consistency in the outputs for all the failure modes sets a working basis for system reliability analysis as discussed in a subsequent section.

The section starts with introducing a practical corrosion model since it is applicable to all the failure modes. The section then covers methods for the four failure modes.

2.2 Corrosion Model. Corrosion reduces the section modulus of the hull of a vessel by thinning the thickness of primary structural members. It reduces the ability of the structure to resist the externally induced bending moment. Several models of general corrosion growth have been suggested [1,6,7]. In the presence of corrosion, the ultimate strength (S_u) of a structural member is given by

$$S_u(t) = \begin{cases} S_{u0} & t \le t_r \\ c(t) S_{u0} & t > t_r \end{cases} \tag{1}$$

where S_u is the ultimate strength (i.e., resistance) of a structural component; t_r is the life of coating (years) as a threshold time; t is the age of the vessel (years), S_{u0} is the initial ultimate strength of a structural component at $t = 0$; $c(t)$ is a strength reduction factor accounting for corrosion of dimensionless nature in the range [0,1], a model that may take the following form:

$$c(t) = 1 - a_1 a_2 (t - t_r)^b \tag{2}$$

where a_1 = annual thickness reduction factor for general corrosion, a_2 = strength reduction factor per unit value of a_1, and b = a model coefficient to account for trend nonlinearity, commonly taken as 1. In the case of fatigue and fracture, the effect of corrosion leads to an increase in the local stresses (S) that can be expressed as follows:

$$S(t) = \begin{cases} S_0 & t \le t_r \\ S_0 / c(t) & t > t_r \end{cases} \tag{3}$$

where S = base stress for fatigue analysis for a particular detail, S_0 = initial base stress for fatigue analysis at $t = 0$, and $c(t)$ = stress reduction factor accounting for corrosion of dimensionless nature in the range [0,1] as provided in Eq. 2.

The model coefficients of Eq. 2 were estimated by analyzing thickness measurements of marine vessels, i.e., two USCG cutters, after 40 years of service. The annual thickness reduction as a percent of the nominal thickness was statistically examined for illustration and the 88th percentile values, i.e., the 5th largest out of 40 years for each cutter, were computed for the thickness reduction as provided in Table 1 for the two cutters. The values in Table 1 are in the form of fractions of nominal thicknesses used in the design and construction of corresponding components. The descriptive statistics of these 88th percentiles are provided in Table 2 with the following values *conservatively* recommended as default values for assessing the structural life of marine vessels (a sampling of well maintained USCG cutters): $a_1 = 0.005$ per year (i.e., the fraction of original thickness per year), and $b = 1$. Also, relationships between buckling strength of stiffened panels and corrosion using parametric analysis were developed as shown in Figs. 1(*a*) and 1(*b*), which accounts for plate buckling, stiffened panel buckling, web buckling, and torsional-flexural buckling. It was observed from these relationships [e.g., Figs. 1(*a*) and 1(*b*)] that the strength drops by amount in the range of 16 to 22% for 10% thickness reduction due to corrosion, i.e., on the average of $(22 - 19)/10 = 1.9$ for average stiffened panel. Therefore, the coefficient a_2 can be set to 0.5 as strength reduction factor per a unit value of a_1. Such a linear relationship (i.e., $a_2 = 0.5$) is reasonably accurate to 30% general corrosion per Fig. 1(*b*), after which it would become nonconservative.

2.3 Reliability of Stiffened Panels and Hulls

2.3.1 Ultimate Strength Including Buckling. Based on reevaluation of 215 tests by various researchers and using an empirical formulation, Herzog [8] developed models for the ultimate strength of stiffened panels that are subjected to uniaxial compression with or without lateral loads. In this paper, the case of uniaxial compression without lateral pressure is presented as an example since the hydrostatic lateral load is relatively small. The ultimate stress F_u of a longitudinally stiffened panel is given by the following empirical model from [8]:

$$F_u = \begin{cases} m\bar{F}_y \left[0.5 + 0.5\left(1 - \frac{ka}{r\pi}\sqrt{\frac{\bar{F}_y}{E}}\right)\right] & \text{for } \frac{b}{t} \le 45 \\ m\bar{F}_y \left[0.5 + 0.5\left(1 - \frac{ka}{r\pi}\sqrt{\frac{\bar{F}_y}{E}}\right)\right]\left[1 - 0.007\left(\frac{b}{t} - 45\right)\right] & \text{for } \frac{b}{t} > 45 \end{cases} \tag{4}$$

in which E = material modulus of elasticity. The average yield strength $\bar{F}_y$ is

$$\bar{F}_y = \frac{F_{ys}A_s + F_{yp}A_p}{A_s + A_p} \tag{5}$$

Table 1 Corrosion summary of 88th percentiles of nominal thickness reduction for two cutters at various locations

Cutter 1: location	Annual thickness reduction[a]	Cutter 2: location	Annual thickness reduction[a]
01 LEVEL WEATHER DECK FR 32-98	0.002341463	01 LEVEL WEATHER DECK FR 32-98	0.002634146
01 WEATHER DECK PORT FR 98 - FR 260	0.002634146	01 WEATHER DECK PORT FR 98 - FR 260	0.00595122
01 WEATHER DECK STBD FR 98 - FR 260	0.003121951	01 WEATHER DECK STBD FR 98-260	0.003609756
MAIN DECK FR 32 - FWD	0.004682927	MAIN DECK FR 32 FWD	0.002536585
MAIN DECK FR 100 - FR 32	0.003512195	MAIN DECK STBD FR 32 - FR 100	0.002146341
MAIN DECK STBD FR 100 - FR 300	0.003317073	MAIN DECK PORT FR 32 - FR 100	0.001365854
MAIN DECK PORT FR 100 - FR 300	0.002439024	MAIN DECK STBD FR 100 - FR 304	0.003512195
MAIN DECK FRAME 300 - AFT	0.004	MAIN DECK PORT FR 100 - FR 304	0.004909218
RESCUE GEAR LOCKER (1-68-3-A)	0.00204878	MAIN DECK FRAME 304 AFT	0.003804878
FOUL WEATHER GEAR LOCKER (1-68-1-A)	0.000195122	DECK GEAR LOCKER (1-68-2-A)	0
GEAR LOCKER (1-68-2-A)	0.001756098	RESCUE GEAR LOCKER (1-68-3-A)	0
VESTIBULE (1-264-1-L & 1-264-2-L)	0.002341463	VESTIBULE (1-264-1&2-L)	0.004780488
FAN ROOM (1-280-1-Q) DECK	0	CIWS MAGAZINE (1-299-1-M) DECK	0
FAN ROOM (2-32-1-Q)	0	FAN ROOM (1-280-1-Q)	0.002731707
BOSN'S WORKSHOP (2-48-2-Q)	0.001853659	FAN ROOM (2-32-1-Q)	0
ET SHOP (2-56-1-A)	0.000682927	ET STORES (2-56-1-A)	0
BOSN'S STOREROOM (3-32-0-A)	0.00204878	BOSN'S WORKSHOP (2-48-2-Q)	0
FLAMMABLE LIQUIDS STOREROOM (3-22-0-K)	0.001658537	BOILER DECK (2-192-0-X)	0.004195122
GYM ROOM (3-48-0-A)	0.000520325	BOSN'S STORES (3-32-0-A)	0.001756098
MACHINE SHOP (3-168-2-Q) & AUXILIARY MACHINERY ROOM NO. 1 (3-179-1-E)	0.008780488	FLAMMABLE STORES (3-22-0-K)	0
AUXILIARY MACHINERY ROOM NO. 3 (3-272-0-E)	0.001636406	GYM ROOM (3-48-0-A)	0.001756098
AUXILIARY MACHINERY ROOM NO. 3 (3-272-0-E) JP-5 TANK TOP	0.009584665	MACHINE SHOP (3-184-2-A)	0.001170732
COMMISSARY STORES (3-280-6-A)	0.003902439	AUXILIARY MACHINERY ROOM NO. 1 (3-179-1-E)	0.001560976
DC STOREROOM (3-336-0-A)	0.003252033	AUXILIARY MACHINERY ROOM NO. 3 (3-272-0-E)	0.001626016
ENGINEERS STOREROOM NO. 2 (3-304-01-A)	0.003382114	COMMISSARY STORES (3-280-6-A)	0.002585366
PUMP ROOM NO. 1 (4-96-0-Q)	0.001560976	DAMAGE CONTROL STOREROOM (3-336-0-A)	0.004227642
SEWAGE TREATMENT ROOM NO. 1 (5-144-0-Q)	0.002585366	ENGINEERS STOREROOM NO. 2 (3-304-01-A)	0.00302439
DIESEL OIL PUMP ROOM (5-192-0-E)	0.001317073	PUMP ROOM NO. 1 (4-96-0-Q)	0.00097561
ENGINE ROOM PORT (5-192-01-M)	0.002439024	SEWAGE TREATMENT ROOM NO. 1 (5-144-0-Q)	0.00204878
ENGINE ROOM STBD (5-192-01-M)	0.003252033	DIESEL OIL PUMP ROOM (5-192-0-E)	0.000390244
76MM MAGAZINE NO. 1 (5-32-0-M)	0.00195122	ENGINE ROOM PORT (5-192-01-M)	0.006292683
TRANSVERSE BULKHEAD 202 LOOKING FWD	0.003239024	ENGINE ROOM STBD (5-192-01-M)	0.009317073
TRANSVERSE BULKHEAD 256 LOOKING AFT	0.003707317	76MM MAGAZINES NO. 1 & NO. 2 (5-32-0-M & 5-48-0-M)	0.000325203
TRANSVERSE BULKHEAD 336	0.001268293	TRANSVERSE BULKHEAD 202	0.00097561
TRANSOM LOOKING AFT	0.001170732	TRANSVERSE BULKHEAD 256	0.003863415
		TRANSVERSE BULKHEAD 336	0.000585366
		TRANSOM	0.000780488

[a]Fraction values of nominal thickness used in design and construction.

Table 2 Descriptive statistics of the 88th percentiles of nominal thickness reduction for two cutters

Statistics	Thickness-reduction fraction value	
	Cutter 1	Cutter 2
Mean	0.002634	0.002309
Standard error	0.00034	0.000352
Median	0.002341	0.001756
Mode	0.002341	0
Standard deviation	0.002013	0.00214
Sample variance	4.05E-06	4.58E-06
Kurtosis	5.197887	1.771212
Skewness	1.925937	1.186615
Range	0.009585	0.009317
Minimum	0	0
Maximum	0.009585	0.009317
Sum	0.092184	0.085439
Count	35	37
Fifth largest	0.003902	**0.00478**
Fifth smallest	0.000683	0
Confidence level (95.0%)	0.000692	0.000713

where F_{yp} = yield strength of plating; F_{ys} = yield strength of stiffener; $A_p = bt$, cross-sectional area of plating; $A_s = t_f f_w + t_w d_w$, cross-sectional area of stiffener; and $A = A_s + A_p$, cross-sectional area of plate-stiffener. The parameter $k = 1.0$, 0.8, or 0.65, corresponding to the following respective end conditions: (1) both ends are simply supported, (2) one end is simply supported and the other is clamped, and (3) both ends clamped. The parameter $m = 1.2$, 1.0, or 0.8 per Herzog [8], corresponds to the following respective cases: (1) no or average imperfection and no residual stress, (2) average imperfection and average residual stress, and (3) average or large imperfection and high value for the residual stress; a = span (length) of stiffener, b = stiffener spacing; t = plate thickness; and r = radius of gyration of one stiffener with fully effective plating and is given by

$$r = \sqrt{\frac{I}{A}} \tag{6}$$

where A = sectional area of the plate and the stiffener and is given by

$$A = bt + d_w t_w + f_w t_f \tag{7a}$$

The moment of inertia of one stiffener with fully effective plating (I) is given by

$$I = \frac{bt^3}{12} + bt\left(z_0 - \frac{t}{2}\right)^2 + \frac{d_w^3 t_w}{12} + d_w t_w\left(z_0 - t - \frac{d_w}{2}\right)^2 + \frac{f_w t_f^3}{12} + f_w t_f\left(z_0 - t - d_w - \frac{t_f}{2}\right)^2 \tag{7b}$$

where z_0 = distance of neutral axis from the base line of plate of the exterior plate surface; t_w = thickness of stiffener web; t_f = thickness

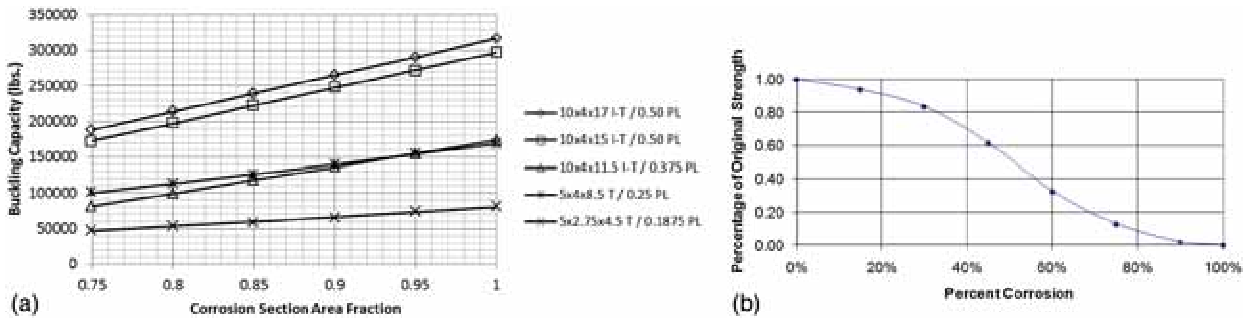

Fig. 1 Effects of corrosion on the buckling strength of a stiffened panel: (*a*) buckling capacity and corrosion area fraction and (*b*) percent of original strength and percent corrosion

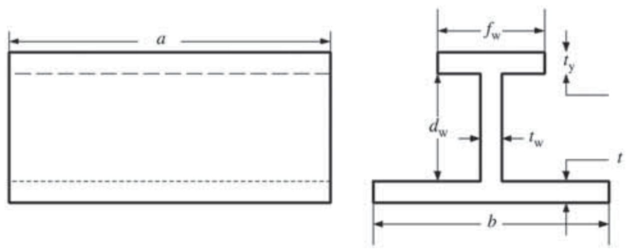

Fig. 2 A stiffened panel

of stiffener flange; d_w = stiffener web height; and f_w = stiffener flange width. The parameter m of Eq. 4 was necessary since the 215 tests evaluated by Herzog belong to three distinct groups. Group I (75 tests) consisted of small values for imperfection and residual stress, Group II (64 tests) had average values for imperfection and residual stress, while the third group (Group III, 76 tests) consisted of higher values for imperfection and residual stress. Figure 2 defines the panel geometry [2].

The Herzog model was compared with experimental and numerical data [9,10,11] and proved to predict the strength value reasonably well. Assakkaf and Ayyub [11] concluded that the empirical model [8] for predicting the ultimate strength of stiffened panels has the least bias with a relatively low coefficient of variation among the other competing models. Table 3 provides the recommended stiffened panel strength model for the load and resistance factor design (LRFD) development [2,11]. The table also shows their probabilistic characteristics and biases.

In cases where the MAESTRO [12] finite-element models (see reference list for information on this computer program) are available for a vessel, the strength of the stiffened panels can be obtained from the MAESTRO [12] models and used as an empirical approximation of the ultimate strength of the panels. In cases where the panels are subjected to tension, the strength can be taken as the yield strength [13] as summarized in Table 3.

As for hulls, the probabilistic characteristics can be based on the MAESTRO [12] model of Table 3 with a bias of 1, a coefficient of variation (COV) of 0.18, and a lognormal probability distribution.

2.3.2 Loads. In this paper, two primary load types are considered: (1) stillwater vertical bending moment and (2) combined wave and dynamic vertical bending moment. Combined vertical and lateral bending can be similarly treated. The stillwater vertical bending can be estimated using fundamental naval architecture principles to obtain a nominal value at any station of interest along a vessel's length. The nominal value and Table 4 can be used to probabilistically characterize this load. The bias for the stillwater vertical bending moment is less than 1, e.g., 0.7, as was reported for combatant vessels. The bias factor might vary significantly, and depend greatly on the use of the vessel.

The computations of the wave bending moments can be based on identification of operational profile, computation of ocean wave statistics, calculation of extreme wave-induced bending moment, and application of the largest extreme wave bending moment in analysis [3]. Michaelson [14] provides a computer program for

Table 3 Recommended stiffened panels strength models for reliability analysis of stiffened panels and hulls

Loading case	Mean (description)	Total bias	Coefficient of variation (COV)	Distribution type	Reference
Uniaxial compression	Eq. (4)	1.0	0.18	Lognormal	Herzog [8]
Uniaxial compression	MAESTRO model	1.0	0.18	Lognormal	MAESTRO [12]
Uniaxial tension	F_y (ordinary steel)	1.11	0.07	Lognormal	Hess et al. [13]
Uniaxial tension	F_y (high-strength steel)	1.22	0.09	Lognormal	Hess et al. [13]

Table 4 Recommended primary loads for reliability analysis of stiffened panels and hulls

Loading type	Mean (description)	Total bias	Coefficient of variation	Distribution type	Reference
Stillwater vertical bending moment	Using fundamental naval architecture (naval vessels)	0.70	0.15	Normal	
Combined wave and dynamic vertical bending moment	A annual load occurrence using SPECTRA	1.0	0.25	Weibull	Michaelson [14]
Combined wave and dynamic vertical bending moment	Annual extreme value	1.0	0.25	Weibull	Ayyub et al. [3]
Load encounter rate	Annual load rate (λ)	NA	NA	Deterministic	

Note: NA = not applicable.

performing these computations, called SPECTRA, that produces annual loading that can be represented by a Weibull probability distribution as provided in Table 4 [15]. The combined wave and dynamic vertical bending moment produced by SPECTRA is for a single encounter, whereas the combined wave and dynamic vertical bending moment [3] is the annual extreme value.

2.3.3 Performance Function and Reliability Assessment. The reliability of a ship structural component can be defined as the likelihood of it maintaining its ability to fulfill its design purpose for some time period under specified environmental and operational conditions. In this paper, calculating time-dependent reliabilities based on its ultimate strength is based on hulls or stiffened panels in a particular region of interest of a vessel. A strength performance function can be expressed in consistent units as follows:

$$g(t) = S_u(t) - L_{sw}(t) - L_w(t) \tag{8}$$

where S_u is the strength of a stiffened panel random variable accounting for all relevant uncertainties, e.g., F_u in Eq. 4; L_{sw} is the stillwater loading random variable accounting for modeling uncertainty in still water; and L_w is the wave loading random variable accounting for modeling uncertainty, nonlinearities, and dynamic effects. Typical values are provided in Tables 3 and 4.

The instantaneous reliability may be obtained based on the limit state defined in Eq. 8, where the failure domain is defined by $\Omega = [g(t) < 0]$ and its compliment $[g(t) > 0]$ defines the safe domain. The instantaneous failure probability at time t is defined by

$$P_f(t) = \int_{\Omega} f(x(t))dx \tag{9}$$

where $f(x(t))$ is the joint probability density function of the basic random variables defining strength and loading random variables at time t. In general, the joint probability density function is unknown, and evaluating the convolution integral is a formidable task. Several practical approaches including the first-order reliability method (FORM), second-order reliability method (SORM), advanced second moment (ASM) method, or Monte Carlo simulation are usually used. The theory of FORM, SORM, and Monte Carlo simulation are well established and can be found in Refs. [16,17]. The initial probability of failure (P_f) at design and construction, i.e., at $t = 0$, is given by Eq. (9) using $t = 0$. The survival probability (P_s) is

$$P_f = 1 - P_s \tag{10}$$

In the presence of degradation mechanisms such as corrosion, the ultimate strength $S_u(t)$ is a decreasing function of time according to Eq. 1; therefore, the probability of failure is also a function of time. By varying the time period t from zero to an expected service life, the decreasing values of ultimate strength $S_u(t)$ can be estimated. Furthermore, the instantaneous failure probability at any time t, defined by $\Omega = [g(t) < 0]$ without regard to survival of a vessel in the previous years, can be obtained using Eq. 9.

Several methods for analytical time-dependent reliability assessment are available. In these methods, significant loads as a sequence of pulses can be described by a Poisson process with mean occurrence rate λ, random intensity L, and duration τ. The treatment is based on reliability theory [e.g., 17] and its subsequent adaptation for strength-degraded structures [18]. The performance function (Z) of a component or system at any instant of time (t) can be defined as

$$Z(t) = S(t) - L(t) \tag{11}$$

where $S(t)$ is the strength at time t and $L(t)$ is the load at time t as shown in Fig. 3. The instantaneous probability of failure at time t can then be defined as the probability of $S(t)$ less than $L(t)$; however, this instantaneous probability treatment does not recognize what has previously happened to the component or system from the start of its life to the present, represented by time t. One is usually interested in the first occurrence of L exceeding S, not the

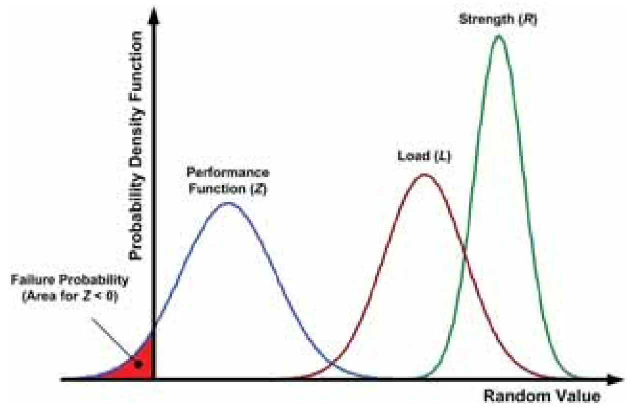

Fig. 3 Probability density functions of resistance *S* and load *L* [25]

instantaneous occurrence, requiring the imposition of a condition on the probability of L exceeding S of being the first time in its life. Such a conditional probability concept is the basis for computing what is termed time-dependent reliability, and estimated using the reliability function $R(t)$.

The reliability function, $R(t)$, is defined as the probability that a component or a system survives during interval of time $(0, t)$ based on a performance function Z. Assuming the load to follow a Poisson process with a rate λ means that the time to a load occurrence is exponentially distributed. Characterizing the time to failure requires not only the time to load occurrence but also the consideration that only some of the load occurrences may lead to failure; therefore, the following expression can be made based on the exponential distribution:

$$R(t) = \exp(-\lambda \hat{P}_f t) \tag{12}$$

where $\lambda\hat{P}_f$ is the product of load rate (λ) and the average failure probability ($\hat{P}_f$) over the period $(0, t)$ that should account for any degradation of the strength (S). The strength degradation, for example due to the corrosion of a structural member, can be modeled by a function $0 < c(t) < 1$ and used as a multiplier to an initial strength (S_0 at $t = 0$.) This probability, $\hat{P}_f$, is taken as the average value over the period $(0, t)$ as follows:

$$\hat{P}_f = 1 - \frac{1}{t}\int_{\tau=0}^{t} P(Z > 0)dt = 1 - \frac{1}{t}\int_{\tau=0}^{t} P(cS > L)dt \tag{13}$$

where $Z = S - L$ is an example performance function. Substituting Eq. 13 into Eq. 12 and accounting for the uncertainty in the initial strength produces the following expression:

$$R(t) = \int_{s=0}^{\infty} \exp\left[-\lambda t\left(1 - \frac{1}{t}\int_{\tau=0}^{t} P(c(\tau)s > L)d\tau\right)\right] f_{S_0}(s)ds \tag{14}$$

where $f_{S_0}(s)$ is the probability density function of the initial strength (S_0). Noting that the expression $P(c(\tau)s > L)$ in Eq. 14 is the cumulative distribution function of L evaluated at $c(\tau)s$, the reliability function can be written as

$$R(t) = \int_{s=0}^{\infty} \exp\left[-\lambda t\left(1 - \frac{1}{t}\int_{\tau=0}^{t} F_L(c(\tau)s)d\tau\right)\right] f_{S_0}(s)ds \tag{15}$$

The reliability can be expressed in terms of the failure rate or hazard function, $h(t)$, as

$$h(t) = -\frac{d}{dt}\ln(R(t)) \tag{16a}$$

which is also related as follows:

$$R(t) = \exp\left(-\int_0^t h(\tau)d\tau\right) \tag{16b}$$

and

$$h(t) = \frac{f(t)}{1 - F(t)} \tag{16c}$$

The reliability $R(t)$ is based on complete survival during the service life interval $(0, t)$. It means the probability of successful performance during the service life interval $(0, t)$. Therefore, the probability of failure, $P_f(t)$ or $F(t)$, can be computed as the probability of the complementary event, $P_f(t) = 1 - R(t)$, not being equivalent to $P[S(t) < L(t)]$, the latter being just an instantaneous failure at time t without regard to previous performance.

The conditional expectation method [17] was implemented based on the following performance function:

$$Z = c(t)S_u - L_{sw} - L_w \tag{17}$$

The computational procedure for the conditional expectation method is as follows:

- In the ith simulation cycle, randomly generate S_u and L_{sw} as s_{u_i} and l_{sw_i}
- Evaluate $R_i(t)$ using Eq. 15 for all the t values of interest, $t = 1,2,3, \ldots 50$ years for each simulation cycle as follows:

— For $t = 1$, evaluate

$$\frac{1}{t}\int_{\tau=0}^{\tau=1} F_{L_w}(c(\tau)s_{u_i} - l_{sw_i})d\tau$$

using the trapezoidal rule based on say 100τ increments, and then compute

$$R_i(t=1) = \exp\left[-\lambda t\left(1 - \frac{1}{t}\int_{\tau=0}^{\tau=1} F_{L_w}(c(\tau)s_{u_i} - l_{sw_i})d\tau\right)\right]$$

— For $t = 2$, evaluate

$$\frac{1}{t}\int_{\tau=1}^{t=2} F_{L_w}(c(\tau)s_{u_i} - l_{sw_i})d\tau$$

using the trapezoidal rule based on 100 additional increments and add the result to the previous one of

$$\frac{1}{t}\int_{\tau=0}^{\tau=1} F_{L_w}(c(\tau)s_{u_i} - l_{sw_i})d\tau,$$

then compute

$$R_i(t=2) = \exp\left[-\lambda t\left(1 - \frac{1}{t}\int_{\tau=0}^{\tau=1} F_{L_w}(c(\tau)s_{u_i} - l_{sw_i})d\tau - \frac{1}{t}\int_{\tau=1}^{\tau=2} F_{L_w}(c(\tau)s_{u_i} - l_{sw_i})d\tau\right)\right]$$

and repeat the process until $t = 50$.

Repeat the previous step for the next simulation cycle $i + 1$ to obtain $R_{i+1}(t)$ for $t = 1,2, \ldots, 50$ and until $I = N$ cycles.

For each t, compute the statistics of $R(t)$ and check for convergence as follows:

$$\bar{R}(t) = \frac{\sum_{i=1}^{N} R_i(t)}{N} \tag{18}$$

where N is the number of simulation cycles. The accuracy of this estimate can be evaluated through the variance (Var) and COV as given by

$$\mathrm{Var}(\bar{R}(t)) = \frac{\sum_{i=1}^{N} (R_i(t) - \bar{R}(t))^2}{N(N-1)} \tag{19}$$

and

$$\mathrm{COV}(\bar{R}(t)) = \frac{\sqrt{\mathrm{Var}(\bar{R}(t))}}{\bar{R}(t)} \tag{20}$$

It should be noted that the composite trapezoidal rule with a uniform grid can be used to calculate the integrals

$$\int_a^b R(x)dx \approx \frac{b-a}{2N}(R(x_0) + 2R(x_1) + 2R(x_2) + \cdots + 2R(x_{N-1}) + R(x_N)) \tag{21a}$$

where $R(x)$ is an arbitrary function, N is the number of intervals for numerical integration, and $x_i = i$th value of x as follows:

$$x_i = a + i\frac{b-a}{N}, \quad \text{for } i = 0,1,2, \ldots, N \tag{21b}$$

2.4 Fatigue Reliability. Fatigue design criteria are typically expressed in years of service, such as 30, 40, or 50 years, without crack initiation with some associated probability. A general design procedure for fatigue can be based on reliability methods [3,4,7,19,20,21,22].

The fatigue life of a structural detail, subjected to the action of cyclic stress, is defined as the total number of stress cycles required to initiate a dominant fatigue crack added to the number of stress cycles required to propagate this crack until the final failure. This total life, in a simplified view, is a function of the geometry of the structure (local and global) applied stress range, the mean stress and the environment where the structure is located.

The stress-based fatigue analysis methodologies, represented by the classical S-N diagram, embody the damage evolution, crack nucleation, and crack growth stages of fatigue into a single, experimentally characterized continuum formulation. These S-N curves, however, are developed experimentally based on relatively small structures and their failure does not necessarily correspond to ship structural failure, which is based on the behavior of very large highly redundant structure. Another factor that could be taken into account in fatigue analysis is the corrosion effect. In simple terms, the corrosion process can cause reduction in plate thickness, making the stress range acting on the structural detail to become time-dependent. This paper presents a method to take into account the effect of corrosion on fatigue reliability assessment using this simplified approach; however, the methodology does not account for corrosion-fatigue interaction. Such interaction should be considered in future studies.

This section provides a method to assess the fatigue life of ship structural details subjected to stress ranges induced by sea loading. That method is based on S-N curve approach for fatigue analysis. The damage associated with fatigue can be calculated as follows:

$$D = \frac{1}{k_S A}\sum_{i}^{k}\frac{n_i}{S_i^b} \tag{22}$$

where k_S expresses the uncertainty in stress range calculation, A is the stress life parameter of the S-N curve; B is the slope parameter of the S-N curve, n_i is the number of actual load cycles at the ith stress range level (S_i), and k is the number of stress range levels. The damage calculated according to Eq. 22 considers that the stress range acting on the structural detail, for each sea state condition, is constant during the ship structural life. Nevertheless, the ship structure can be corroded during its life.

The corrosion effect, based on the hypothesis of uniform corrosion of ship structural detail, is represented by a reduction of structure thickness, which affects the stress range magnitude and consequently the accumulated fatigue damage. The increase in the local stresses (S) can be expressed by Eq. 3 using the corrosion model of Eq. 2.

Based on Eq. 22, the fatigue damage becomes dependent on the time variation of the stress range due to corrosion effects. The fatigue damage is calculated as follows:

$$D_j = \sum_{j=1}^{T} \frac{1}{k_S A} \sum_{i=1}^{k} \frac{n_{i1}}{S_{ij}^b} \tag{23}$$

where T is the number of operational years considered in the analysis, n_{i1} is the number of actual load cycles at the ith stress range level (S_i) during one operational year, k is the number of stress range levels, and S_{ij} is the ith stress range level during one operational year calculated as follows:

$$S_{ij} = \frac{S_i}{(1 - a_1 a_2((j-1) - t_r)^b)}, \quad \text{for } j > (t_r + 1) \tag{24a}$$

$$S_{ij} = S_i, \quad \text{for } j \le (t_r + 1) \tag{24b}$$

According to Eq. 23, the fatigue damage must be calculated annually and the total fatigue damage at the end of the operational period (T) is the sum of the annually calculated fatigue damage.

The performance function for fatigue analysis can be expressed as follows:

$$g = \Delta_L - D_j \tag{25}$$

where Δ_L is the fatigue damage ratio limit that has a mean value of 1 [23]. The method takes into account the corrosion damage effect according to Eq. 2.

2.5 Fracture Distribution and Reliability. The reliability method developed herein is based on the crack growth prediction executed according to linear elastic fracture mechanics principles, where the stress intensity factor (K) is used to define the stress field in the vicinity of a crack. The value of the stress intensity factor depends on the loading, body configuration, crack shape, and mode of crack displacement. According to Fuchs and Stephens [24], the basic equation that governs crack growth, named the Paris law, is given by

$$\frac{da}{dN} = C \Delta K^m \tag{26}$$

where a is the crack size, N is the number of fatigue cycles, ΔK is the range of stress intensity factor, and C and m are crack propagation parameters that come from fracture mechanics.

The range of the stress intensity factor is given by [24]

$$\Delta K = S f(a) \sqrt{\pi a} \tag{27}$$

in which $f(a)$ is a function of crack geometry and structure geometry and S is the stress range induced by the cyclic loading. When the crack size a reaches some critical crack size a_{cr}, failure is assumed to have occurred.

Although most laboratory testing is typically performed with constant amplitude stress ranges, Eq. 26 is always applied to variable stress range models that ignore sequence effects. Rearranging the variables in Eq. 26 and substituting Eq. 27 into Eq. 26, the number of cycles for the crack to grow from the initial size (a_i) to a particular crack size (a) can be computed by integration as follows:

$$N = \frac{1}{C(S)^m} \int_{a_i}^{a} \frac{da}{f(a)^m (\sqrt{\pi a})^m} \tag{28}$$

Modeling $f(a)$ as a constant for a particular structural detail with an assumed geometry, the crack growth prediction can be expressed by integrating Eq. 28 ([25]) up to $a = a_f$:

$$a_f^{(1-\frac{m}{2})} = a_i^{(1-\frac{m}{2})} + \left(1 - \frac{m}{2}\right) C k_S^m S^m \pi^{\frac{m}{2}} \alpha^m N_{\text{Fracture}} \tag{29}$$

The random variables are a_i, k_S, and C. The probabilistic characteristics of those random variables are provided by Ref. [25]. The stress range is considered deterministic. The value N_{Fracture} represents the number of loading cycles during an operational life. The final crack size distribution (a_f) is also a random variable with a distribution that can be simulated with the application of Monte Carlo simulation. The statistical properties of a_f, such as mean, median, and COV can be calculated from the simulation results.

The stress fluctuation during a ship's operational life due to sea state conditions requires modifying Eq. 29 to account for the planning time horizon of interest that can be different than the built-in number of operational days in typical sea-state databases. The crack growth analysis is modified as follows:

$$a_f^{(1-\frac{m}{2})} = a_i^{(1-\frac{m}{2})} + \left(1 - \frac{m}{2}\right) C k_S^m \pi^{\frac{m}{2}} \alpha^m \sum_{i=1}^{k} \frac{T_{\text{operational}}}{T_{\text{database}}} N_i S_i^m \tag{30}$$

where $T_{\text{operational}}$ represents the operational life for crack growth analysis (in days) according to the planning time horizon, T_{database} represents the number of days used to define the stress range database for a particular sea state, N_i is the frequency of occurrence of the ith stress range (S_i) recorded in the database, and k is the number stress ranges defining the underlying histogram.

The crack growth analysis produces the final crack size (a_f) distribution for a particular operational life based on the input of the probability distribution functions of a_i, k_S, and C, and the parameter α related to the crack geometry and structural detail. Prediction of the probability distribution of a_f enables engineers to consider appropriately consider repair and maintenance decisions, and assigning vessels to new missions.

The following computation procedure based on Monte Carlo simulation is proposed:

- In the ith simulation cycle, generate the random variables a_i, C, and k_S according to their respective probability distributions.
- Use the generated values of a_i, C, and k_S, and deterministic values of m, α, S_i, N_i, the summation over k, $T_{\text{operational}}$ and T_{database} to compute a_f for the times $t = 1,2,3, \ldots,$ the number of years in the planning horizon, e.g., 30 years.
- Terminate the ith simulation cycle either by reaching the number of the years in the planning horizon or once the time-dependent $a_f(t)$ exceeds the permissible crack size, e.g., 0.25 in.
- Repeat the simulation process N times.
- Store the generated values of a_i, C, and k_S, and crack size a_f as a function of time t and for each simulation cycle.

The postprocessing of the stored results has the objectives of characterizing the crack size histogram as a function of time t, and estimating the reliability function $R(t)$. The following procedure is proposed:

- For each time t, using an increment of 1 year and up to the number of the years in the planning horizon, compute the count of values (denoted n_t) out of N simulation cycles, average, median, standard deviation, and coefficient of variation of a_i, C, and k_S, and crack size a_f.
- For each time t, using an increment of one year and up to the number of the years in the planning horizon, estimate the reliability function $R(t)$ as the count of values out of N simulation cycles divided by N, i.e., n_t/N, and compute the cumulative distribution function of life $(F(t)) = 1 - R(t)$.
- Estimate the statistical uncertainty of the estimated reliability by its COV as follows:

$$\mathrm{COV}(R(t)) = \frac{\sqrt{R(t)(1-R(t))/N}}{R(t)} \quad (31)$$

The COV values of Eq. 31 treat the simulation cycles as Bernoulli trials [16], and they approach 0 as N approaches infinity. The COV can be used as a criterion to determine the required number of simulation cycles (N) to accurately estimate $R(t)$.

3 System Reliability Analysis

The system reliability can be analyzed using a model of discrete components. The proposed method is based on the assumption of a discretized system in a series composed of n components, i.e., the system is considered to perform adequately, if and only if all of its n components are performing adequately. Figure 4 depicts a reliability block diagram representation of a series system consisting of three components.

With the reliability (R) defined as $1\text{–}P_f$, the time-dependent reliability function of a series system composed of n components, $R_s(t)$, is given by

$$R_s(t) = \prod_{i=1}^{n} R_i(t) \quad \text{for independent events} \quad (32)$$

The component reliability values are obtained using the methods described in previous sections. The system reliability can be evaluated for any group of components that represent a subsystem or a system of interest, such as a bulkhead, a deck, a station, or the entire vessel. Equation 32 is based on the assumption that the failure events of the components are independent. For the case of perfect, positive dependence among failure events of components, the minimum value of all the component reliabilities is the value that should be assigned to $R_s(t)$ as follows:

$$R_s(t) = \min_{i=1}^{n} R_i(t) \quad \text{for perfect dependence} \quad (33)$$

For the purposes of system reliability evaluation of stiffened panels, the condition of independence is closer to reality than perfect dependence, and is assumed in the system reliability computations for stiffened panels, although the real level of dependence falls in between these two extreme cases. For the purposes of system reliability evaluation relating to fatigue, the condition of perfect dependence is considered closer to reality than independence, and is assumed in the system reliability computations for fatigue, although the real level of dependence falls in between these two extreme cases. As for computing system reliability of the hull structure including both cases of stiffened panels and fatigue details of interest, the respective system reliability results for stiffened panels and fatigue details as systems can be combined based on the assumption of a system in series with independent events. Bounding methods for system reliability assessment are used to examine the effects of independence and perfect, positive dependence [17].

The computational procedure proposed for aggregating component reliability function for the purpose of estimating the system reliability function requires defining the following notations:

R	reliability
t	time
R_{ss}	reliability of a group of stations or an entire vessel as a system
R_{si}	reliability of station i as a system
R_{sp}	reliability of several panels as a subsystem in station j
R_{sft}	reliability of several fatigue details as a subsystem in station j
R_{sfr}	reliability of several fracture details as a subsystem in station j
R_{pj}	reliability of panel j as a component
R_{ftj}	reliability of fatigue detail j as a component
R_{frj}	reliability of fracture detail j as a component
R_{hi}	reliability of hull girder station i

The models and associated assumptions are summarized in Table 5 where the asterisk (*) means arithmetic multiplication at corresponding times for $R(t)$.

While the method for the systems analysis combines the reliability results at the component level, their individual contributions should be compared along with their respective consequences in a risk assessment framework based on the user's risk metrics and risk tolerance. The development of a comparative approach for risk assessment is the subject of further work.

4 Examples

In this section, three examples are used to illustrate the computations for panel buckling failure, fatigue, and fracture.

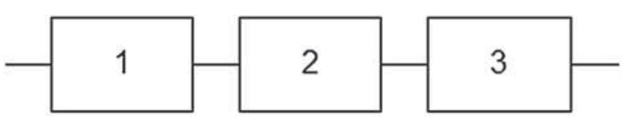

Fig. 4 Series system composed of three components

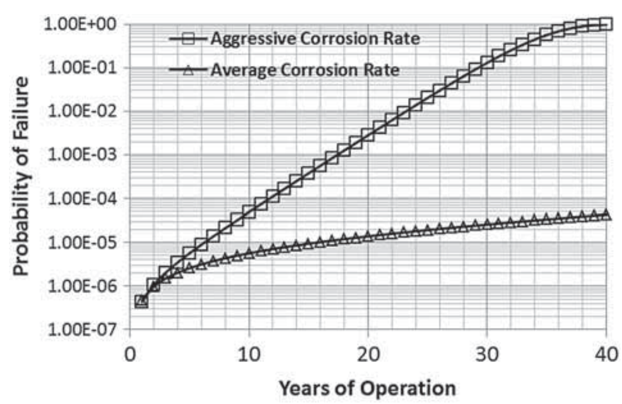

Fig. 5 Effects of corrosion rate on panel reliability based on buckling strength

Table 5 Assumptions and models for discretized system reliability analysis

Item	Computation order	Independent	Perfectly positively correlated	System in series	System in parallel	Model
Panels within a vessel's station	1	x		x		$R_{sp} = R_{p1} * R_{p2} * \ldots$
Fatigue	2		x	x		$R_{sft} = \min(R_{ft1}, R_{ft2}, \ldots)$
Fracture	3		x	x		$R_{sfr} = \min(R_{fr1}, R_{fr2}, \ldots)$
Hull girder station i	4	x		x		R_{hi}
Within station i	5	x		x		$R_{si} = R_{sp} * R_{sft} * R_{sfr} * R_{hi}$
Several stations or an entire vessel	6	x		x		$R_{ss} = R_{s1} * R_{s2} * \ldots$

x = assumption employed.

Table 6 Assumed parameters for the fatigue illustrative example

Variable	Parameter or comments	Value
Fatigue damage limit (D)	Mean	1.0
	COV	0.3
	Distribution type	Lognormal
Stress uncertainty factor (k_s)	Mean	1.0
	COV	0.1
	Distribution type	Lognormal
Analysis time planning horizon in days (years)	Deterministic	18250 (50)
Sea load condition	Cutter Specific Load Histogram from the SPECTRA (Michaelson [14]) code in the SLASH library	NP_G-4 (general North Pacific environment)
S-N curve	SLASH code library	AASHTO_D

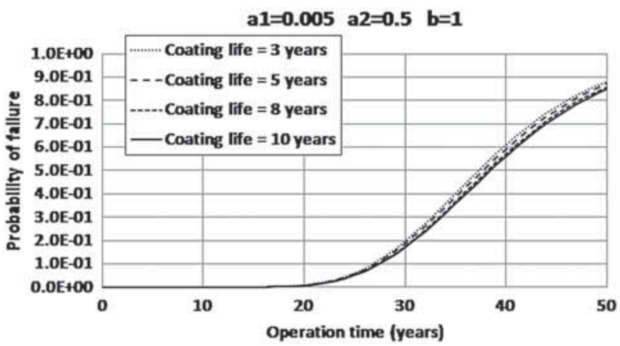

Fig. 6 Effect of corrosion on probability of fatigue failure for a structural detail

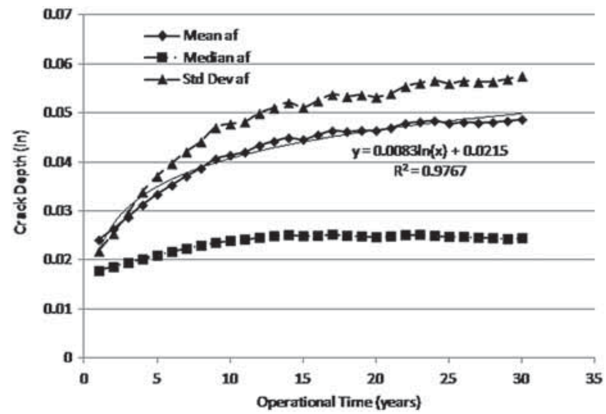

Fig. 7 Mean, median, standard deviation, and fitted crack depth (a_f) to the mean as functions of years of operation

4.1 Example 1: Panel Buckling and Corrosion. Figure 5 provides the results for the panel buckling with the average corrosion shown in Table 2 and parameters shown in Table 3. In the figure, the aggressive corrosion is ten times the average value and occurs in isolated areas in the structure due to standing water that are difficult to inspect. The results in Fig. 5 indicate the coating systems are generally effective. The areas with the highest probability of failure are associated with aggressive corrosion. It can be inferred from Fig. 5 that aggressive corrosion can be managed in a five-year inspection schedule to reduce the risk of significant failure. However, class-wide, targeted inspections and maintenance are required to reduce the risk associated with aggressive local corrosion.

4.2 Example 2: Fatigue Life Prediction With Corrosion. Table 6 and Fig. 6 illustrate the computations of the probability of failure of a structural detail with corrosion. The analysis is performed for an assumed sea load condition and S-N curve AASHTO-D. The probability function parameters for fatigue damage limit and stress uncertainty are present in Fig. 5. The corrosion model parameter a_1 was arbitrarily set equal to 0.005 for demonstration purposes of the proposed model that accounts for corrosion effects in fatigue reliability and life. Clearly, the life of coating threshold time has a strong influence in fatigue reliability.

4.3 Example 3: Trend Prediction of Crack Size Distribution. An illustrative example was prepared for the purposes of this report using an example sea load condition and crack growth curve proposed by Lassen [25,26]. The stress uncertainty is modeled by a normal distribution with a mean equal to 1.0 and COV of 0.1. The crack is modeled as semi-elliptical (in a structural panel) with the relation (a/c) equal to 0.1 that leads to α equal to 1.10 [25] in fracture mechanics analysis. The initial crack depth distribution is assumed to follow an exponential probability distribution with a mean value of 0.025 in. The structural detail thickness is assumed to be 0.25 in. The analysis considers the depth growth of the crack along the ship operational life.

Figure 7 shows a prediction of the mean value of crack depth as a function of the ship's operational use in years using Eq. 30. A model was fitted to the mean crack depth as shown on the same figure. Figure 8 shows the histograms of final crack depth for different operational times based on the simulation results. The simulation limits the maximum crack depth to the structural detail thickness. The longer the operational life, the greater the likelihood that the crack becomes a through thickness crack, i.e., the probability of exceeding the 0.25-in. limit increases with the increase in the operational time as shown in Fig. 9 in terms of a reliability function $R(t)$.

5 Structural Life Assessment of Ship Hulls

The Fatigue Life Assessment of Ship Structures (FLASH) methodology was implemented using a web-enabled computer code and database to compute the time-dependent reliability functions at the component and system levels. The tool calculates the structural reliability function based on time to first failure at the component and system levels for hull girders, stiffened panels, and fatigue by accounting for degraded strength due to corrosion, and fracture. SLASH requires specification of the basic random variables for the corresponding performance functions for ship structure failure modes.

SLASH includes a database to manage users, ships, and associated stations, components, details, and results. Navigation is handled through tabs and highlighted links. Each tab or link corresponds to a specific action required for analysis of a ship. A tab for ship system definition provides tools for defining a ship through stations. Each station can be further expanded into a hull girder,

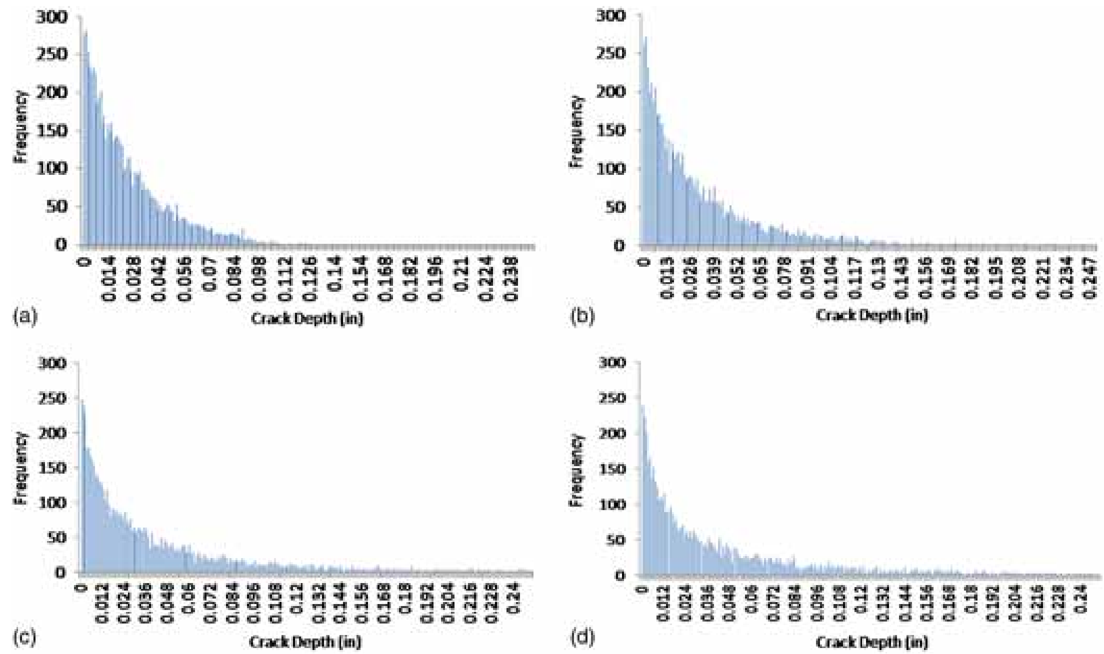

Fig. 8 Crack depth histograms as a function of years of operation: (*a*) After one year of operation, (*b*) after five years of operation, (*c*) after ten years of operation, and (*d*) after 15 years of operation

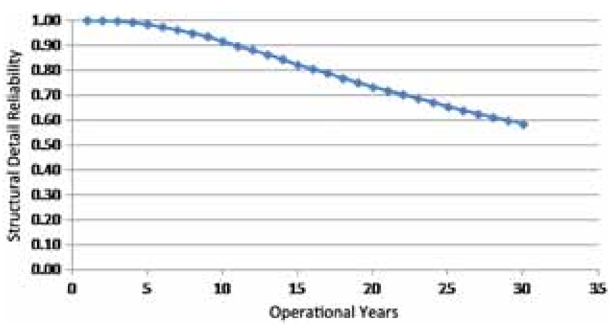

Fig. 9 Fatigue reliability as a function of years of operation

stiffened panels, and fatigue profiles for each panel. Tabs are also present to examine each station's components individually as well as an additional tab to define fracture characteristics. Figures 10 and 11 illustrate the screens used for database access and management.

An analyze option for created ship elements allows the user to mathematically define the appropriate characteristics of the model. Input is handled through drop-down menus and text fields. User-defined quantities include deterministic factors for defining corrosion and fatigue models. A library of predefined load histograms and S-N curves are available for fatigue calculations. Values for probabilistic analysis including distribution type, corresponding parameters, and analysis types can also be set as shown in Fig. 12. An option to update quantities for existing elements is available

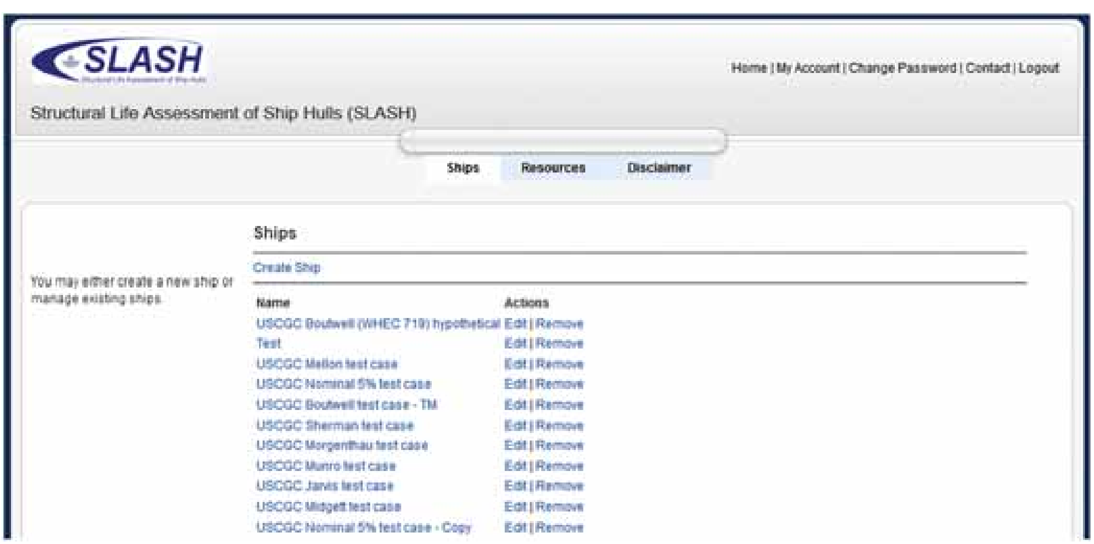

Fig. 10 SLASH ship database

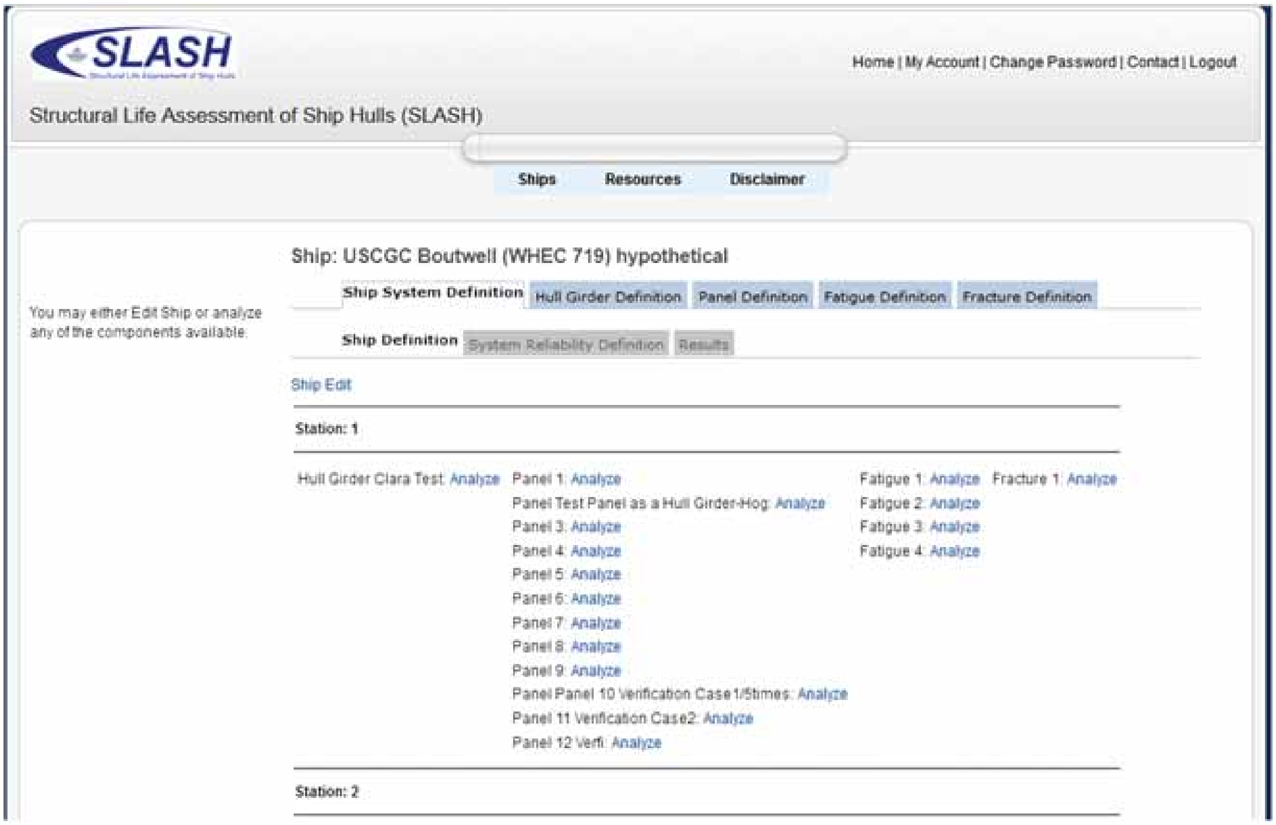

Fig. 11 SLASH ship definition tab

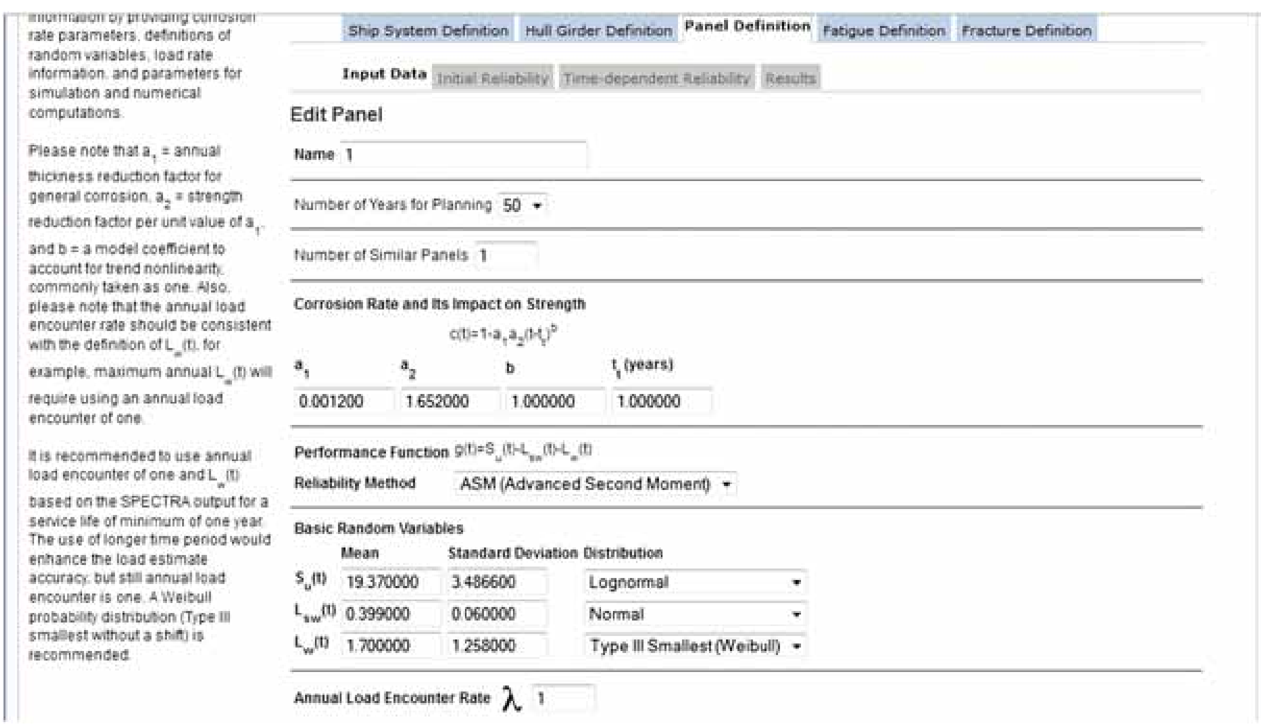

Fig. 12 Example SLASH input screen

Station	Components	Results	
		Time-dependent probabilities (reliability (R) and failure probability (Pf) as a function of time)	
Station 1	Hull Girder Clara Test	R(0): 6.58108004e-01	P(0): 0.341892
		R(1): 7.26592611e-01	P(1): 0.273407
		R(2): 5.59921356e-01	P(2): 0.440079
		R(3): 4.51827357e-01	P(3): 0.548173
		R(4): 3.77173957e-01	P(4): 0.622826
		R(5): 3.24086860e-01	P(5): 0.675913
		R(6): 2.84370717e-01	P(6): 0.715629
		R(7): 2.53408298e-01	P(7): 0.746592
		R(8): 2.28842679e-01	P(8): 0.771157
		R(9): 2.08490393e-01	P(9): 0.79151
		R(10): 1.92191428e-01	P(10): 0.807809
		R(11): 1.12202666e-01	P(11): 0.887797
		R(12): 4.12454477e-02	P(12): 0.958755
		R(13): 1.51655479e-02	P(13): 0.984834
		R(14): 5.58536787e-03	P(14): 0.994415
		R(15): 2.05323738e-03	P(15): 0.997947
		R(16): 7.56167765e-04	P(16): 0.999244
		R(17): 2.77600880e-04	P(17): 0.999722
		R(18): 1.02225528e-04	P(18): 0.999898
		R(19): 3.76030391e-05	P(19): 0.999962
		R(20): 1.38315925e-05	P(20): 0.999986
System		R(0): 6.58108004e-01	P(0): 0.341892
		R(1): 7.26592611e-01	P(1): 0.273407
		R(2): 5.59921356e-01	P(2): 0.440079
		R(3): 4.51827357e-01	P(3): 0.548173
		R(4): 3.77173957e-01	P(4): 0.622826
		R(5): 3.24086860e-01	P(5): 0.675913
		R(6): 2.84370717e-01	P(6): 0.715629
		R(7): 2.53408298e-01	P(7): 0.746592
		R(8): 2.28842679e-01	P(8): 0.771157
		R(9): 2.08490393e-01	P(9): 0.79151
		R(10): 1.92191428e-01	P(10): 0.807809
		R(11): 1.12202666e-01	P(11): 0.887797
		R(12): 4.12454477e-02	P(12): 0.958755
		R(13): 1.51655479e-02	P(13): 0.984834
		R(14): 5.58536787e-03	P(14): 0.994415
		R(15): 2.05323738e-03	P(15): 0.997947
		R(16): 7.56167765e-04	P(16): 0.999244
		R(17): 2.77600880e-04	P(17): 0.999722
		R(18): 1.02225528e-04	P(18): 0.999898
		R(19): 3.76030391e-05	P(19): 0.999962
		[illegible]	[illegible]

Fig. 13 Example SLASH output

through the *Analyze* function or alternatively through specific *Update* links for each element. The execution of the SLASH program corresponding to a ship element of interest is available under the Analyze menu. Results of the most recent execution of the SLASH program are stored in a Results tab to avoid the necessity to re-execute SLASH to view results.

The individual results (see Fig. 13) for each ship component are tied together for each station through the ship definition. Stations are analyzed by aggregating the effects of the individual components defined for each station. A total ship reliability result is calculated by combining the reliabilities of each station. Results are also presented as reliability plots by year for each station defined for the ship. For additional information on this tool, the authors may be contacted.

6 Summary and Conclusions

This paper provides the technical background on the approach developed for assessing the time-dependent reliability functions for marine vessels within the context of the strength of hulls, stiffened panels, fatigue, and fracture. This analysis supports decision making for maintenance, operation and repair as part of fleet support, and hull structural life evaluations. Moreover, the assessment can be used as a basis for making statements relating to the fatigue life to probability of failure for a critical location, groupings of similar details, and the entire vessel. It is envisioned that such methods will be used to perform probabilistic life assessments of vessels in support of designing new vessels and the prediction of remaining life of vessels in operation.

Acknowledgment

The authors would like to acknowledge the financial support of the U.S. Coast Guard and the technical support of its naval architects at the Surface Forces Logistics Center. The authors also acknowledge the assistance of Ms. Clara Popescu Brooks and Dr. William McGill. Methods and results presented in this paper are the opinions of the authors and do not represent the opinions of the U.S. Coast Guard. The views expressed herein are those of the authors and are not to be construed as official or reflecting the views of the Commandant or of the U.S. Coast Guard.

References

[1] Paik, J. K., Kim, S. K., and Lee, S. K., 1998, "Probabilistic Corrosion Rate Estimation Model for Longitudinal Strength Members of Bulk Carriers," Ocean Eng., **25**(10), pp. 837–860.

[2] Assakkaf, I., Ayyub, B. M., Hess, P., and Atua, K., 2002, "Reliability-Based Load and Resistance Factor Design (LRFD) Guidelines for Stiffened Panels and Grillages of Ship Structures," Naval Eng. J., ASNE, **114**(2), pp. 89–111.

[3] Ayyub, B. M., Assakkaf, I., Kihl, D. P., and Sieve, M. W., 2002, "Reliability-Based Design Guidelines for Fatigue of Ship Structures," Naval Eng. J., ASNE, **114**(2), pp. 113–138.

[4] de Souza, G. F. M., and Ayyub, B. M., 2000, "Probabilistic Fatigue Life Prediction for Ship Structures Using Fracture Mechanics," Naval Eng. J., ASNE, **112**(4), pp. 375–397.

[5] Ayyub, B. M., 2010, *Structural Life Assessment of Ship Hulls (SLASH), Report Prepared for U.S. Coast Guard Naval Architecture Branch*, Baltimore, MD.

[6] Orisamolu, I. R., Brennan, D. B., and Akpan, U. O., 1999, "Probabilistic Modeling of Corroded Ship Structural Panels," Presented at the 8th CF/CRAD Meeting on Naval Application of Materials Technology and Inter-Naval Corrosion Conference, Halifax, Nova Scotia, Canada.

[7] Akpan, U. O., Koko, T. S., Ayyub, B. M., and Dunbar, T. E., 2002, "Risk Assessment of Aging Ship Hull Structures in the Presence of Corrosion and Fatigue," Marine Struct., **15**(3), pp. 211–232.

[8] Herzog, A. M., 1987, "Simplified Design of Unstiffened and Stiffened Plates," J. Struct. Eng., ASCE, **113**(10), pp. 2111–2124.

[9] Paik, J. K., and Lee, J. M., 1996, "An Empirical Formulation for Predicting the Ultimate Compression Strength of Plates and Stiffened Plates," Trans. Soc. Naval Architects of Korea, **33**(3), pp. 8–21 (in Korean).

[10] Paik, J. K., and Thayamballi, A. K., 2002, *Ultimate Limit State Design of Steel-plated Structures*, John Wiley & Sons, Chichester, UK.

[11] Assakkaf, I., and Ayyub, B. M., 2004, "Comparative and Uncertainty Assessment of Design Criteria for Stiffened Panels," J. Ship Research, Soc. Naval Architects Marine Eng., **48**(3), pp. 231–247.

[12] MAESTRO Version 8.9, *Optimum Structural Design, Inc.*, DRS C3 Advanced Technology Center.

[13] Hess, P. E., III, Bruchman, D. D., Assakkaf, I. A., and Ayyub, B. M., 2002, "Uncertainties in Material Strength, Geometric and Load Variables," Naval Eng. J., ASNE, **114**(2), pp. 139–165.

[14] Michaelson, R., 2000, User's Guide for SPECTRA: Version 8.3, *NSWCCD Report TR-65-2000/07*, March 2000.

[15] Sikora, J. P., Michaelson, R., and Ayyub, B. M., 2002, "Assessment of Cumulative Lifetime Seaway Loads for Ships," Naval Eng. J., ASNE, **114**(2), pp. 167–180.

[16] Ayyub, B. M., and McCuen, R. H., 2011, *Probability, Statistics and Reliability for Engineers and Scientists*, Chapman & Hall/CRC Press, Boca Raton, FL.

[17] Ayyub, B. M., 2003, *Risk Analysis in Engineering and Economics*, Chapman & Hall/CRC Press, Boca Raton, FL.

[18] Ellingwood, B. R., and Mori, Y., 1993, "Probabilistic Methods for Condition Assessment and Life Prediction of Concrete Structures in Nuclear Plants," Nuclear Eng. and Design, **142**, pp. 155–166.

[19] White, G. J., and Ayyub, B. M., 1987, "Reliability-Based Fatigue Design for Ship Structures," Naval Eng. J., ASNE, **99**(3), pp. 135–149.

[20] Sieve, M. W., Kihl, D. P., and Ayyub, B. M., 2000, Fatigue Design Guidance for Surface Ships, CARDEROCKDIV-U-SSM-65- / Sep. 2000, Naval Surface Warfare Center, Carderock Division, NAVSEA, U. S. Navy, 64 pp.

[21] Stambaugh, K. A., Leeson, D. H., Lawrence, F., Hou, C.-Y., and Banas, G., 1992, "Reduction of S-N Curves for Ship Structural Details," Report SSC 369, Ship Structure Committee, U.S. Coast Guard, Washington, D.C.

[22] Stambaugh, K. A., Lawrence, F., and Dimitriakis, S., 1994, "Improved Ship Hull Structural Details Relative to Fatigue," Report SSC 379, Ship Structure Committee, U.S. Coast Guard, Washington, D.C.

[23] Ayyub, B. M., and McGill, W. L., 2007, *Fatigue Life Assessment of Ship Structures (FLASH)*, U. S. Coast Guard Naval Architecture Branch, Engineering Logistic Center, 2410 Hawkins Point Road, M/S 25, Baltimore, MD.

[24] Fuchs, H. O., and Stephens, R. I., 1980. *Metal Fatigue in Engineering*, John Wiley & Sons, New York.

[25] Ayyub, B. M., and de Souza, G. F. M., 2012, "Structural Detail Assessment of Ship Hulls (SLASH): Fracture Mechanics," Report prepared for U.S. Coast Guard Naval Architecture Branch, Baltimore, MD.

[26] Lassen, T., and Sorensen, J. D., 2002, "A Probabilistic Damage Tolerant Concept for Welded Joints. Part 1: Data Base and Stochastic Modeling," Marine Structure, **15**, pp. 599–613.